EKSPLOATACJA I NIEZAWODNOŚĆ MAINTENANCE AND RELIABILITY

Eksploatacja i Niezawodnosc – Maintenance and Reliability

Volume 23 (2021), Issue 1

journal homepage: http://www.ein.org.pl

Article citation info:
Podulka P. Fast Fourier Transform detection and reduction of high-frequency errors from the results of surface topography profile measurements of honed textures. Eksploatacja i Niezawodnosc – Maintenance and Reliability 2021; 23 (1): 84–93, http://dx.doi.org/10.17531/ein.2021.1.9.

Indexed by: Web of Science Group

Fast Fourier Transform detection and reduction of high-frequency errors from the results of surface topography profile measurements of honed textures

Przemysław Podulka

Faculty of Mechanical Engineering and Aeronautics, Rzeszow University of Technology, ul. Powstancow Warszawy 8, 35-959 Rzeszów, Poland

Highlights

- The approach for detection and reduction of selected measurement errors is presented.
- Power spectral density and autocorrelation function are valuable in noise analysis.
- For minimisation of effect of measurement errors the 'noise surface' is defined.
- Profile analysis might be more valuable than areal when measurement noise is assessed.
- Fast Fourier Transform is useful in definition of high-frequency measurement noise.

Abstract

In this paper, various type of noise detection procedures with surface topography profile analysis were proposed, compared (studied) and suggested. The honed cylinder liner surface textures with additionally burnished oil pockets were measured with a stylus or optical approaches. Measurement errors, defined as high-frequency measurement noise, were taken into sufficient consideration. It was proposed to select the noise detection methods more with profile (2D) than areal (3D) assessments; some-frequency noise was much easier to observe in profile than surface analysis. Moreover, applications of various type of regular filtration methods, mostly based on Gaussian functions, were compared with Fast Fourier Transform filtration for detection or reduction of some (high) frequency-defined measurement errors.

Keywords

surface topography, measurement, measurement errors, measurement noise, cylinder liner, oil pocket, dimple, valley, texture features.

1. Introduction

Measurement and analysis of surface topography (ST) are highly advantageous in assessments of tribological performance of 'engineering surfaces' [17], especially wear resistant [6], lubricant retention, sealing, friction, material contact in general [25]. ST is created in the last stage of the machining process; besides, medium-scale components of ST, waviness, in particular, arise as a result of imperfection in the manufacturing process [21].

Detailed information about ST can be obtained by measurements and analysis of the received raw data. Results in the assessment of wear behaviour of selected surface textures are fraught with many factors that can affect the accuracy of the research carried out. In general, errors in the analysis of ST, dedicated mainly for tribological elements, can be classified as errors in measuring equipment and environment [2], the measured object errors, software [30] or measuring method errors [37]. While considering the measurement uncertainty, it can be grouped in errors: typical for measuring methods [24], those caused by digitisation process [23], another received when data processing is accomplished [26] and other errors [20, 29, 44].

There can arise a few problems in the processing of raw measured data. Usually, the ST parameters of car engine parts are calculated after form (errors of shape and waviness) removal [32]. Errors of this type of data processing can be especially visible when edge-area of two-process textures are considered [28]. Improper selection of form removal procedure can cause classification of properly made parts as a lack and their rejections [31].

ST measurement equipment is often roughly divided into the stylus and non-contact methods [40]. In defiance of significant development of optical techniques, a stylus profilometer is still the most common roughness measuring device in the mechanical industry [22]. Contrary to stylus (contact, in general) methods which are robust but slow optical methods are fast but deeply sensitive to external effects. In general, optical methods require the isolation of instruments from the external environment, which is a complicated task to be accomplished. Therefore, the results of measurement of a rough surface can be fraught by errors caused by the noise occurrence. The noise has different sources, including those generated internally, and those defined as external sources received from the environment.

There are many types of noise in surface metrology, e.g. scattering [43], background [14], measurement/instrument [4], outlier [41], static [9] and other noise-like [1] errors. The measurement noise can be briefly described as the noise added to the output signal [12] occurring when the normal use of measuring instrument is accomplished. The effect of noise occurrence was minimised with various methods, e.g. correlogram correlation [16], by proposals of limitation and matching of bandwidth for various instruments [3], some optimisation approaches for selected (coherence scanning interferometry) measuring

E-mail addresses: P. Podulka - p.podulka@prz.edu.pl

methods [7], the frequency de-noising technique based on the wavelet decompositions [5], Fourier reduction or random phase exclusion schemes [8], and other plenty methods [27].

Widely used in surface texture characterisation is the Fast Fourier Transform (FFT) [18]. The FFT technique is likely to play an important role in the analysis of dry contact of the rough surface [35], contact assessments in general [19]. For example, the power values of power spectral density (PSD) for the atomic force microscopy (AFM) digital data were determined by the FFT algorithms instead of the root-mean-square (rms) and peak-to-valley value when a surface morphology of pentacene thin films and their substrates were considered [15]. Moreover, peak detecting algorithm that combines the white-light phase-shifting interferometry (WLPSI) method and FFT coherence-peak-sensing technique was proposed, which could accurately determine the local fringe peak and improve the vertical resolution of the measurement [39]. Application of this type of algorithm could effectively reduce the batwing effects at the edges and solve the problem of positioning error in the maximum modulation.

FFT can also be associated with other filters, e.g. Gaussian [38], for measurement of surface roughness of optical thin films; the surface profile was obtained by the fringe pattern analysis using the FFT method. Besides, the asperity radius of curvature and asperity density, which are generally derived from a rough surface simulation with FFT, are the two essential parameters for statistical contact model [11]. The simulated rough surface with desired parameters was widely used as an input for the numerical simulation of tribological behaviour such as the asperity contact, lubrication, and wear. Gaussian rough surfaces with desired autocorrelation function (ACF) and spatial statistical parameters, including skewness (*Ssk*) and kurtosis (*Sku*), was developed by combining the FFT, translation process theory, and Johnson translator system [42]. An FFT algorithm can also reduce computational time in the calculation of universal spline filter. Furthermore, for practical use, an improved method prior to the FFT algorithm can be proposed to suppress the end effect [45].

In some cases, the FFT was considered to be one of the essential tools of digital signal processing for surface profiles filtration and was compared with the existing methods [33]. Moreover, a fast white-light interference method for measuring surface depth profiles at nanometer scales was also provided with FFT appliances. White-light profilers have relied either on path difference scanning or on spectral analysis of the reflection from a fixed interferometer. It was shown that, by performing this spectral analysis with an imaging Fourier transform spectrometer, the high speed of spectral techniques might be successfully combined with the simple data interpretation characteristic of a used scanning method [10]. A two-dimensional FFT technique was also proposed for accelerating the computation of scattering characteristics of features on surfaces by using the discrete-dipole approximation; FFT reduced the execution time of data processing as well [36].

In this paper, the FFT filtration method was proposed for detection and reduction of high-frequency measurement errors. It was suggested to analyse the ST with the profile (2D) instead of areal (3D) assessments. A number of profiling techniques have been developed for measuring the topography of rough surfaces [34]. Nonetheless, there is still a grave problem with the selection of procedure for detection of measurement noise. The influence of noise-separation methods on areal and profile ST analysis was not comprehensively studied in previous researches as well.

2. Analysed materials, measurement process and applied methods

In this paper, the honed cylinder liner texture with dimples created by the burnishing techniques was taken into account. They were measured by the stylus instrument, Talyscan 150.The nominal tip radius was about 2 μm, height resolution 10 nm and the measured area 5 mm by 5 mm (1000 x 1000 measured points), sampling interval was 5 μm.

Detection of noise, especially with high-frequency, from the results of raw measured data, was performed with FFT application. The FFT approach was provided for areal (3D) details but in many cases the results were presented for profiles (2D) only. It was caused by the more direct (visible) results in profile detection and reduction of the high-frequency measurement errors by analysis of the PSD and AFC graphs. For each type of surface texture (whereas topography contains the deep/wide dimple or not), the noise-detection procedure was modified to provide the best fits.

The effect of ST feature distribution on noise detection and reduction was carefully studied. Results were compared with those received by regular filtering methods, e.g. Gaussian (GF), robust Gaussian (RGF) or Spline filters (SF). Furthermore, analysis of the power spectral density and the autocorrelation function graphs were accomplished. The PSD was defined with no other functions, e.g. Zoom Factor equal to 1, Loops (number of iterations) also, the smoothing or windows functions were not provided as well. PSDs were received by the support of a commercial software. The noise removal results were also defined as the results of S-operator filtering, described in details previously in surface measurement (ISO) standards.

3. Results and discussions

3.1. Areal and profile analysis of measurement noise

Considering the measurement errors, especially the high-frequency measurement noise (HFMN), it is necessary to describe it along with the associated measurement bandwidth. When HFMN was scrutinised, the PSD of measured detail has been carefully examined, explicitly taking into account the existence of the high-frequencies (frequencies of small scales) on the analysed graph. Moreover, visual detection of HFMN of both contour map plots and PSD graphs from the results of the measurement process was dependent on the width and depth of the ST features.

It was assumed that the size of dimples (valleys) additionally burnished on the honed cylinder liner texture has a significant impact on the noise detection process. In Figure 1, contour map plot of cylinder liner, measured with various velocity (a – 0.2 mm/s and b –1 mm/s), was presented. It was found that if the width (depth) of the considered feature was greater than 0.1 mm (0.010 mm) the HFMN detection was exceedingly difficult or it was infeasible with PSD graph analysis, and there were no required (high) noise-frequencies on the diagrams. The occurrence of deep/wide features on the analysed detail made the visual (eye-view) noise detection enormously complicated.

It was also proposed to compare optical disclosure of HFMN for detail before (raw measured data) and after form removal. 'Flat' surface analysis might give more convincing results than details with higher amplitude (containing form and waviness) when measurement noise was detected with visual PSD plot assessment. The form was eliminated with the application of least-square fitted polynomial plane of 3rd degree enhanced by the valley excluding method. This form separation approach was investigated and substantially confirmed by the previous studies, the usefulness of the applied scheme for characterisation of two-process cylinder liner topographies containing (relatively) large dimples was noticeably improved.

When the mentioned PSD diagrams were visually compared (c and d example against the a and b, from Figure 1), there was no discrepancy (or they were negligible) between the results obtained. Consequently, it was reasonably assumed that detection of HFMN by the analysis of the PSD graph of honed cylinder liner topographies including oil reservoirs, was not reasonably precise regardless of areal form removal process was completed or not. Notwithstanding the previous, the effect of form removal on noise identification (and vice

versa) was not thoroughly scrutinised; nevertheless, this was not one of the underlying assumptions of the conducted research.

Similar problems in optical detecting of the noise from the results of surface texture measurement were obtained with profile (2D) analysis. In Figure 2, profiles (and respectively their PSD diagrams) extracted from honed cylinder liner topography, measured with different speed, were presented. Differences in measurement results were mainly (easy) noticeable with visual analysis of profile plots. Nevertheless, the variations on the PSD graphs were trifling or did not exist. In the considered profile, the valley depth and width were around 30 µm and 0.5 mm, respectively.

It was also assumed that when the number (density) of valleys in 2D (3D) analysis increased, the PSD-detection of HFMN became utterly impracticable. Subsequently, the process of noise disclosure, based on the PSD diagram assessment, appeared to be not precisely stated when honed cylinder liner topographies were studied with valley assays.

The effect of noise amplitude, not analysed in these studies, was also extraordinarily difficult to determine. In further research, where defining of error amplitude would be the primary task, the feature (e.g. valley, dimple) size (and density) and its distribution (considering as well the distance between each of them) might be of great importance. Moreover, the noise identification with PSD assessment was even more complicated that the noise was not visible for each measurement condition (velocity). Additionally, HFMN was discernible with visual profile analysis in contrast to the PSD graph assays for each surface texture measurement velocity.

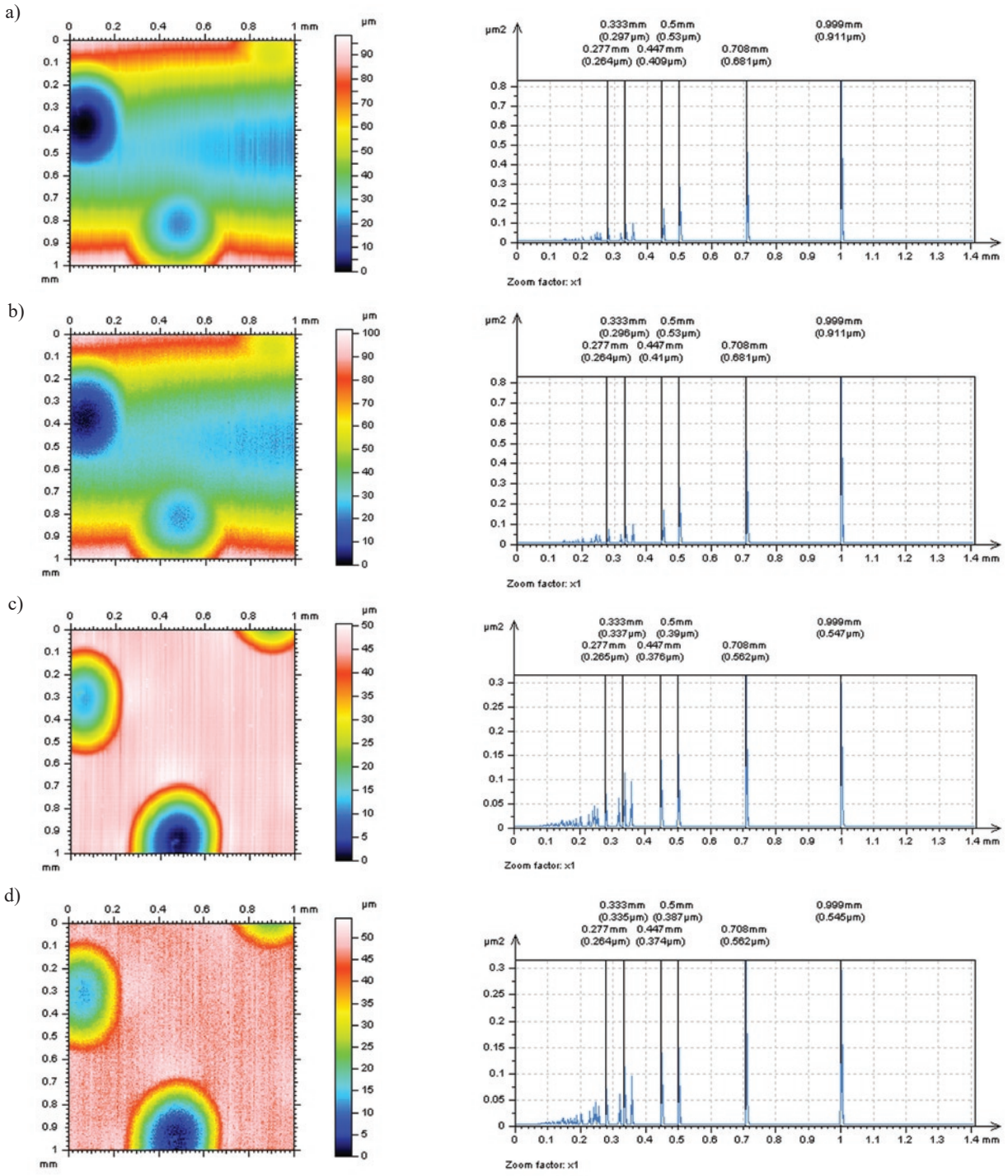

Fig. 1. Contour map plots and PSDs of cylinder liner texture containing wide dimples, measured by stylus instrument with a velocity equal to 0.2 mm/s (a, c) and 1 mm/s (b, d); raw measured data after levelling process (a, b) and texture after form removal by a polynomial of 3rd degree with valley excluding method approach (c, d)

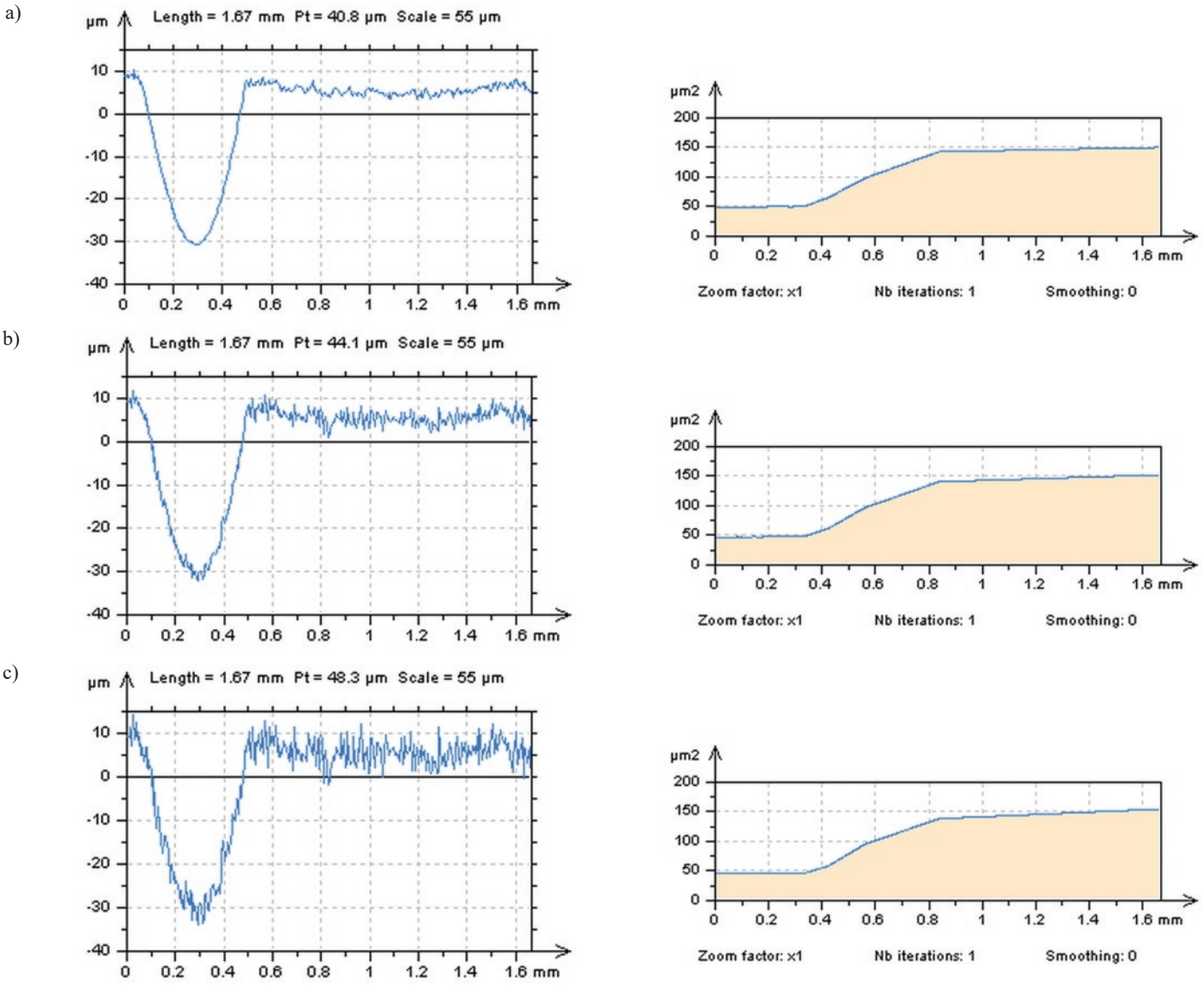

Fig. 2. Profiles and their PSDs respectively, extracted from cylinder liner texture containing one wide dimple, received for stylus measurement with speed equal to (a) 0.2 mm/s, (b) 0.5 mm/s and (c) 1 mm/s

3.2. The effect of feature (dimple) size on the detection of high-frequency measurement errors

The impact of feature (dimples, valley) size (width, depth) on detection of HFMN from the results of raw measured data was taken into consideration; the number (density) of valleys was not studied. It was assumed that for honed cylinder line textures containing dimples with a depth greater than 10 µm, the detection of HFMN with PSD analysis was severely impeded. The smallest valley depth was found the more accurate PSD-identification of measurement noise was observed. In Figure 3, three different profiles (containing dimples with various depth) extracted from honed cylinder liner topography are introduced. As it was assumed in the previous section, in condition when the valley depth was greater than 10 µm, the detection of HFMN with PSD analysis became unattainable (a, b). However, when the dimple depth was smaller than the previously specified value, the noise (high) frequencies were found in the PSD diagram (c). This valley-depth value should be identified for *Sq* of both the surface and the noise (HFMN specifically). Despite that, the arbitrarily selected values should not be decisive; it is suggested to identify the noise occurs in the measurement results by PSD analysis with out-of-deep-feature (out-of-deep-valley/out-of-deep-dimple to be more precise) characteristics. This finding can be entirely appropriate if the noise amplitude is relatively small, concerning the surface height (for both methods – out-of-dimple scheme and approach based on excluding the valleys).

Not only the depth of the surface features affects the PSD-accuracy of noise detection. It was fount that if the depth of valleys was relatively small (usually smaller than Sq/Rq value of non-dimple detail/profile), the HFMN was also challenging to be discerned. The direct impact of dimple width can be clearly designated by the consideration of feature width (A) against the width of out-of-feature detail/profile (B); the description was appropriately introduced in Figure 4. Each profile was shortened to reduce the A/B coefficient. The size of out-of-feature (dimple) profile detail was equal to 0.85 mm, and correspondingly, the width of the valley was decreased from 0.15 mm (a) to 0.05 mm (c), or its value was negligible (d). Consequently, when the value of A/B factor decreased, the PSD-identification of HFMN occurrence increased. In general, when the width of the feature (A) was smaller than 10% of profile width (A + B), then the noise PSD-disclosure increased; visual detection of HFMN was facilitated.

3.3. Reduction of noise from the results of surface topography measurements

Once the procedure of (high-frequency) noise detection is applied, the selection of approach for reduction (removal) of measurement errors should be chosen very attentively. The final selection of noise

reduction procedure has basically the considerable influence on the calculation (values) of areal surface topography parameters. Properly accomplished measurement process might not provide desired (adequate) results when the processing of received raw measured data is not performed competently. The method of reduction of HFMN is, in addition to the form removal procedure, one of the main factors that can cause a false estimation of detail properties and its classification as a lack and rejection.

For reduction of the effect of measurement errors on values of areal surface texture parameters, the FFT filtering was compared with commonly-used (mostly available in commercial software of measuring equipment) algorithms. Several approaches for noise reduction issue were proposed separately. Basically, the HFMN can be defined by analysis of the obtained results with the S-filtering process [13], e.g. regular Gaussian, spline or FFT methods. In the previous research, it was found that the procedure of reduction of HFMN can be selected by assessment of received data from the filtering approach. The results of S-filtering process can be defined as a noise surface (NS) or noise profile (NP), in this specific instance, when the 3D or, correspondingly, 2D measured data were considered. It was also found that NS (NP) received by the S-operation should be consist of only the high-frequencies or those (high) frequencies should be described as an overwhelmingly 'dominant' frequencies. Simultaneously, the frequencies that are required to be removed should be those dominant in the results of noise reduction (filtering as a considered case) procedure. In general, the more dominant frequencies are those with high-frequency spectrum the better results of HFMN reduction process are received.

From the analysis of PSDs of profiles from honed surface texture after reduction of HFMN, it was assumed that the most dominating high-frequency was found for the results obtained after S-filtering by the FFT method. In Figure 5, profiles and their PSDs were presented for profiles after various type of filtering approaches. From Gaussian schemes (GF or RGF), robust filtering caused a greater amplitude of received NP than the regular filter. When the FFT approach was applied, the high-frequencies were those 'dominant'; the amplitude of those frequencies (on PSD graph) was greater than for profiles after noise reduction by other methods (GF, RGF and SF). The amplitude

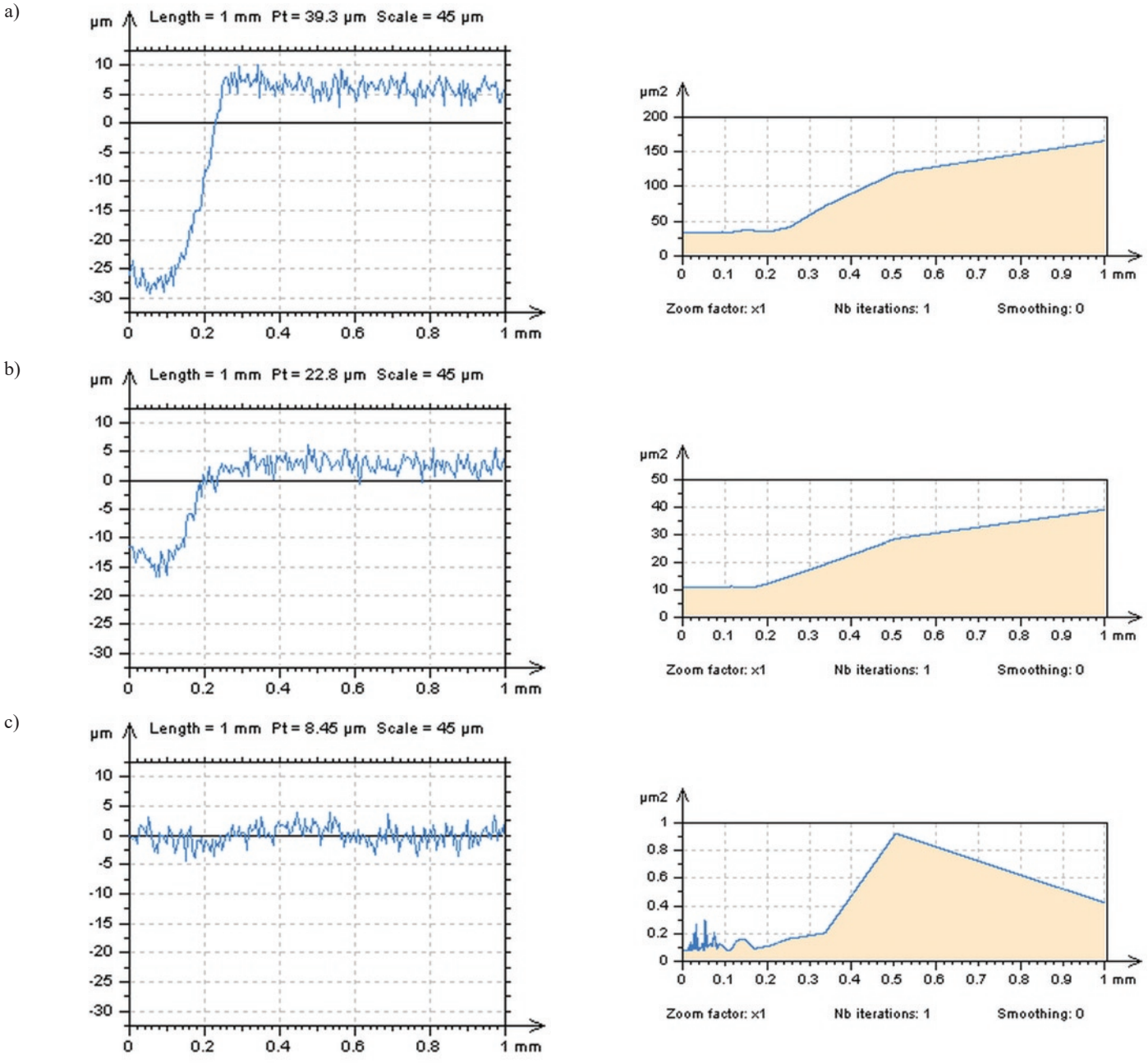

Fig. 3. Profiles and their PSD graphs correspondingly, extracted from plateau-honed cylinder liner texture measured by stylus method with a velocity equal to 0.6 mm/s; profile with deep (depth equal to 35 µm approximately) valley (a), profile with a relatively not-deep (20 µm) valley (b) and non-dimple profile (c)

(maximum height) of received NP was the greatest when RGF was used. Nonetheless, the amplitude of HFMN (NS) was not considered in this paper.

Some features located on the ACF graph (Figure 6) occurred in periodic sentence when commonly available (Gaussian or spline) filters were applied. Received frequencies were more 'periodic' than those after noise reduction by the FFT approach. Moreover, the peak density of ACF also increased when FFT filtering was accomplished instead of generally used filters. The process of noise reduction in profile analysis can be found by definition and assessment of dominant frequency. Additionally, when HFMN was considered to be removed

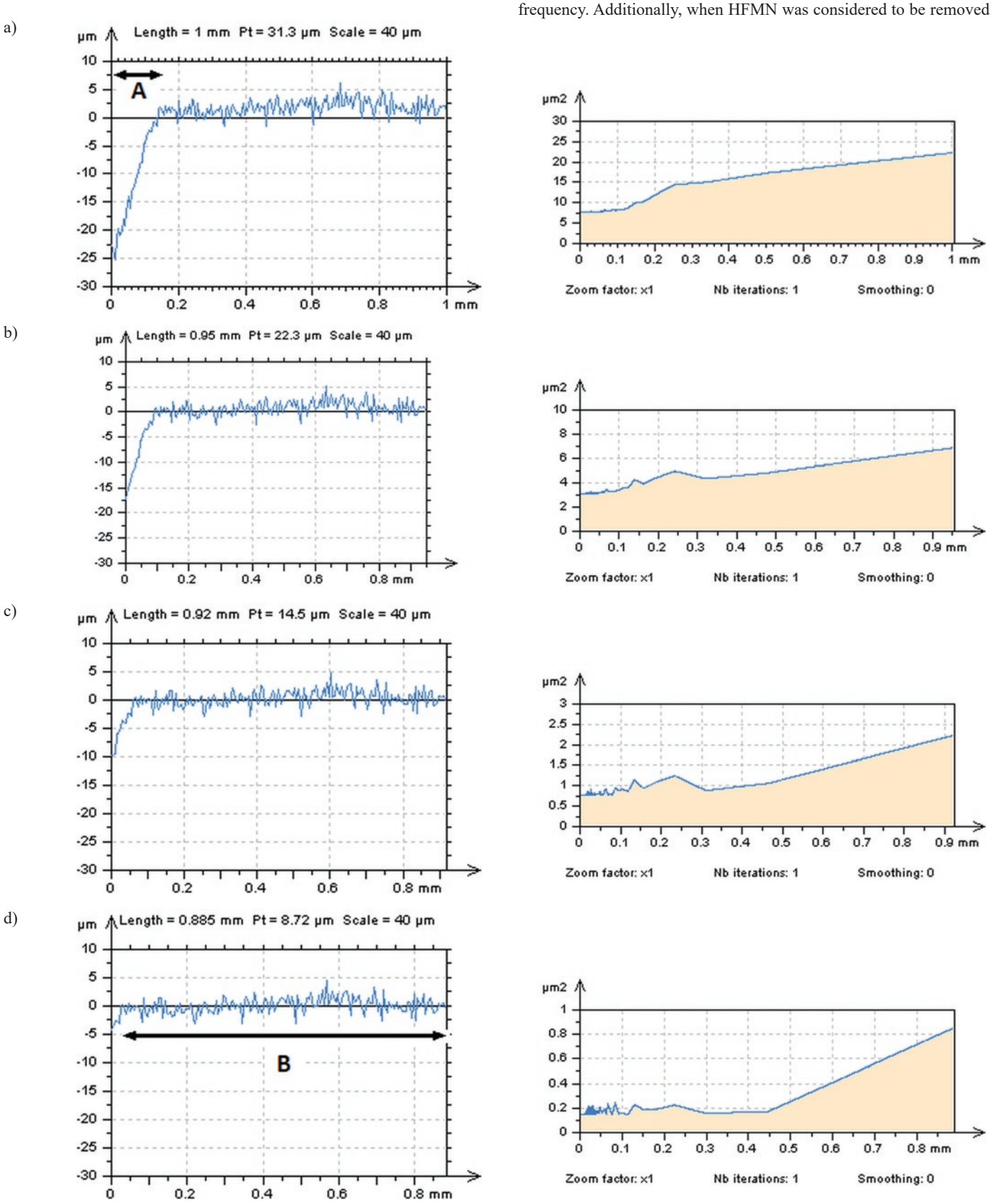

Fig. 4. Profiles, and their PSD graphs correspondingly, extracted from plateau-honed cylinder liner texture measured by stylus method with a velocity equal to 0.7 mm/s; profile with A-size (width) of dimple equal to 0.15 mm (a), 0.1 mm (b), 0.05 mm (c), and non-dimple profile (d)

(minimised), the dominant frequency (high- in particular) should not be found in the received post-processing (after S-operator filtering) data. The smallest amplitude of dominant (removed) frequency was established in the received de-noised data the highly advantageous of the applied algorithm was clearly indicated.

HFMN was removed by application of various filter with a bandwidth equal to 0.015 mm, 0.025 mm and 0.035 mm to improve the utility of FFT approach; nevertheless, studies can be extended to the other values depending on the type of surface texture analysed. For all of the considered cut-off values, the amplitude of dominant (high-) frequency was maximised (minimised) according to the regular filter, when the PSDs of received (NP) results were observed (Figure 7).

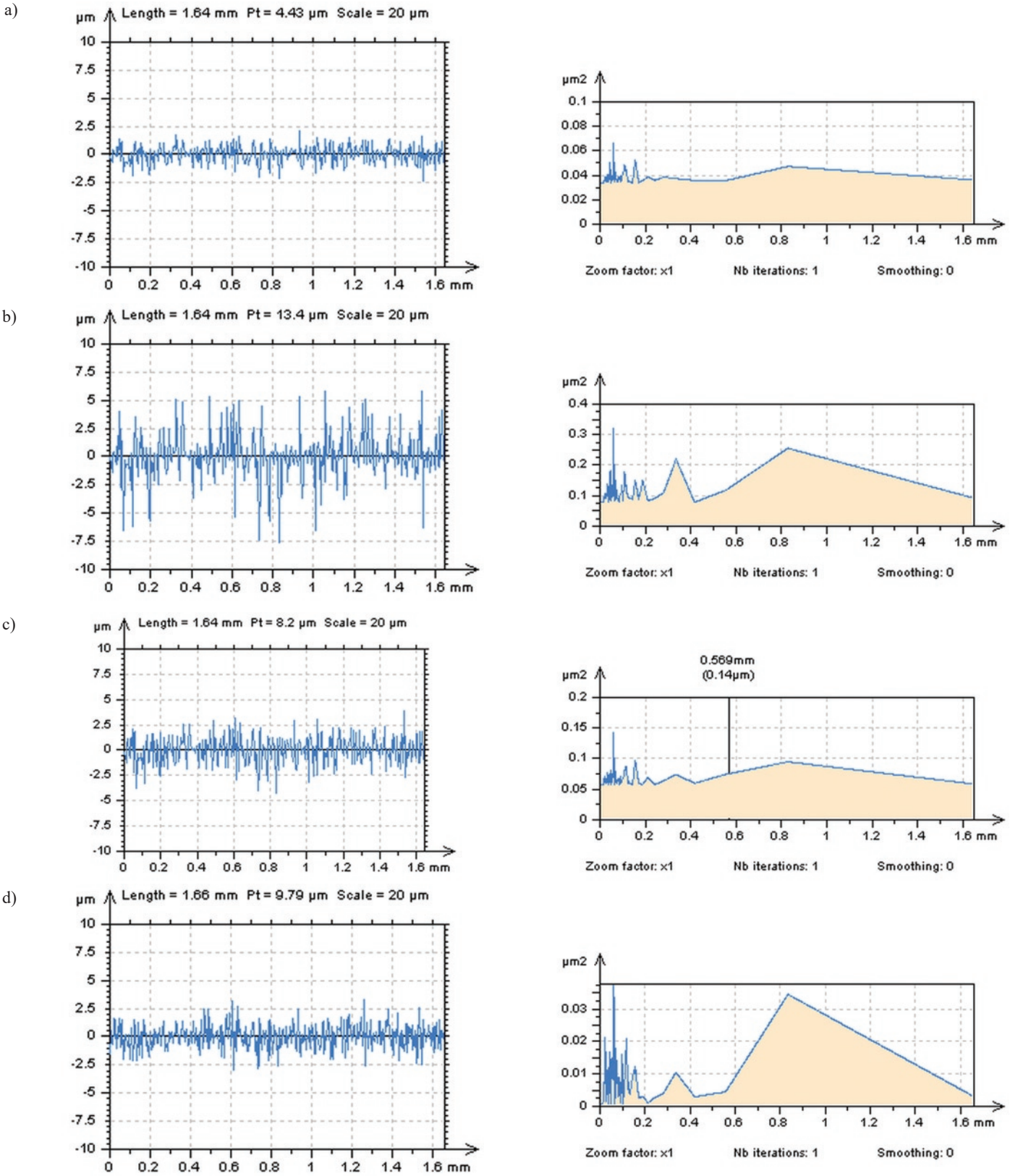

Fig. 5. NPs and its PSDs correspondingly, measured with speed equal to 0.8 mm/s from plateau-honed cylinder liner texture, and after reduction of HFMN by GF (a), RGF (b), SF (c) and FFT (d), cut-off = 0.015 mm

a)

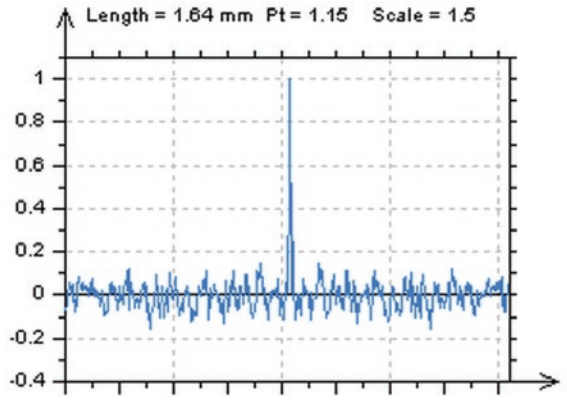

b)

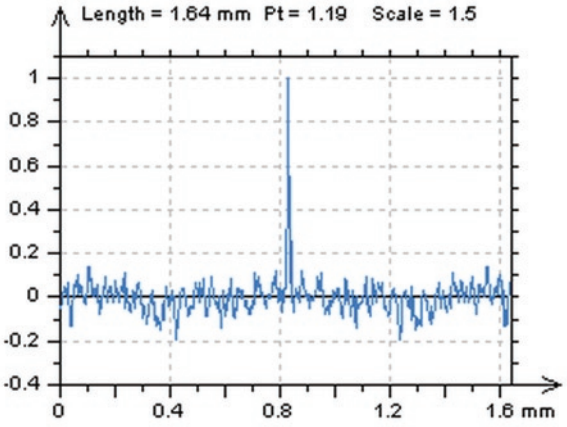

c)

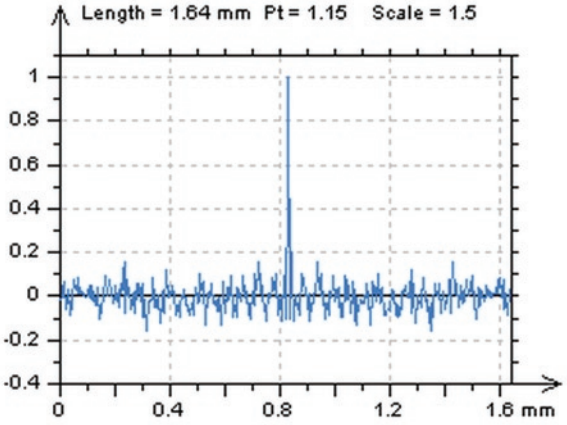

d)

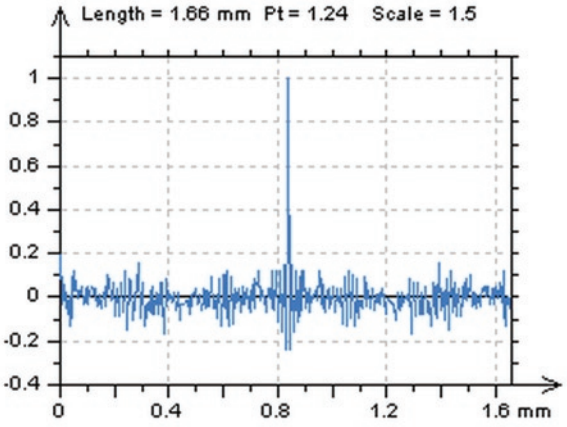

Fig. 6. ACFs of NP, received from measured profile (speed 0.8 mm/s) of honed surface texture obtained after removal of HFMN by GF (a), RGF (b), SF (c) and FFT (d) method with cut-off = 0.015 mm

4. Conclusions

The detection and then reduction of high-frequency measurement noise is a highly demanding task that makes the analysis of surface topography reasonably intuitive. Nonetheless, some applications might be accepted:

1. For honed cylinder liner textures (plateau-honed in particular) containing additionally burnished oil-reservoirs (dimple, valley, wholes in general), the high-frequency measurement noise was exceedingly difficult to detect for areal analysis with power spectral or autocorrelation function applications.

a)

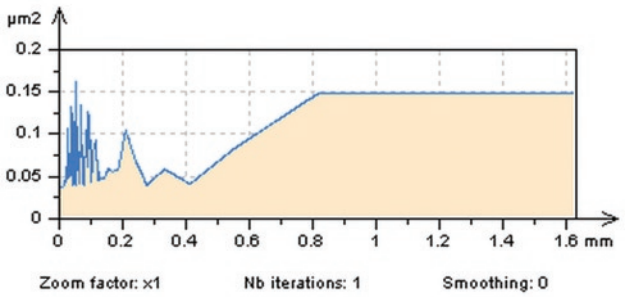

b)

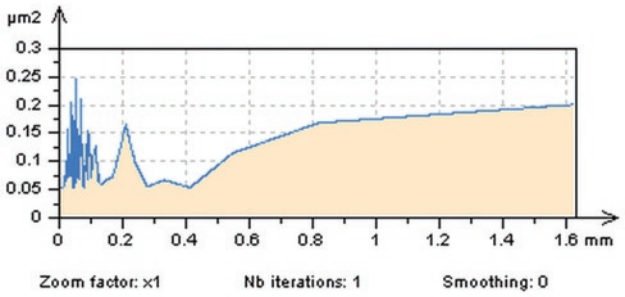

c)

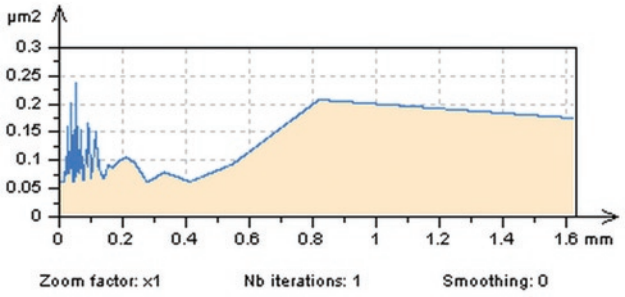

d)

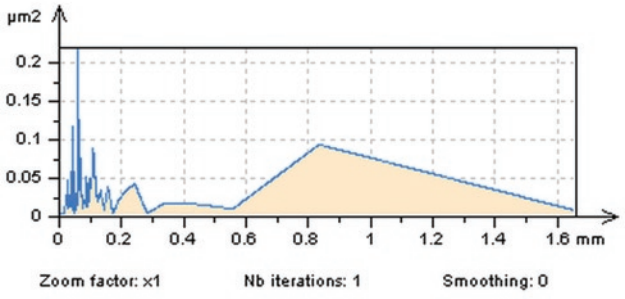

Fig. 7. PSDs of measured profile (speed 0.8 mm/s) from honed surface texture obtained after removal of HFMN by GF (a), RGF (b), SF (c) and FFT (d) method with cut-off = 0.035 mm

The eye view assessment of the occurrence of high-frequency errors in the results of surface topography measurements was increasingly complicated when texture contains some deep features.

2. The form (e.g. cylindrical) of analysed detail has no impact on the process of 'power spectral density' (PSD) detection of high-frequency measurement noise. The differences in PSD graphs, calculated for both raw measured data and data after application of the process of areal form removal (e.g. least-square fitted polynomial plane of 3rd order improved by valley excluding method approach), were imperceptible.
3. It is suggested to identify the noise in the results of surface texture measurement by power spectral density analysis of out-of-feature (deep valleys in particular) details. This might be entirely justified when the noise amplitude is relatively small, according to the surface amplitude (height). Moreover, when the number (density) of valleys in profile (areal) analysis increased, the detection of high-frequency measurement noise, with the analysis of power spectral density graphs, appeared to be infeasible.
4. The feature (dimple) size has a considerable influence on the accuracy of the noise detection procedure. As it was assumed, when the depth of valley was greater than 10 μm (usually when *Sq* of the non-dimple area was smaller than 10% of the *Sq* value calculated for all measured detail – containing dimples), the detection of high-frequency measurement errors (with power spectral density analysis certainly) became unobtainable. In addition, when the width of the feature was also smaller than 10% of the profile width, then the precision of noise disclosure increased.
5. It was suggested to determine the high-frequency measurement noise with noise profile analysis, as a results of S-filtering methods. The properly obtained noise profile should contain only the 'unwanted' (with high-frequency spectrum) components. It was suggested that the removed frequency should be this dominant in the received results after the S-filtering of noise profile.
6. When the received noise profile (surface) were considered with autocorrelation function, it was found that properly defined noise profile (surface) should not contain any periodic waveforms; the noise profile (surface) should be non-periodic (isotropic), in general.
7. For reduction of high-frequency noise from the results of measurement of surface topography, the fast Fourier transform (FFT) was proposed. When compared with commonly-used procedures (e.g. various Gaussian or spline filters) with various cut-off values (e.g. 0.015 mm, 0.025 mm, 0.035 mm), the amplitude of dominant (required high-) frequency was maximised.
8. It is recommended to select the noise reduction procedure with multivariate analysis, combining the profile (areal) eye view (of contour map/profile plots) analysis with assessments of the graphs of power spectral densities and autocorrelation functions.

Acknowledgements

The author kindly acknowledges the Polish National Science Centre for financial support, project number: 2013/09/N/ST8/04333.

References

1. Creath K, Wayant JC. Absolute measurement of surface roughness. Applied Optics 1990; 29(26): 3823-3827, https://doi.org/10.1364/AO.29.003823
2. Dagnall H. Exploring Surface Texture. Rank Taylor Hobson Limited, Leicester, UK, 1986.
3. De Groot P, DiSciacca J. Surface-height measurement noise in interference microscopy. In: Proceedings of SPIE 10749, Interferometry XIX, 2018, 107490Q-7, https://doi.org/10.1117/12.2323900
4. De Groot P. The meaning and measure of vertical resolution in optical surface topography measurement. Applied Sciences 2017; 7(1): 54, https://doi.org/10.3390/app7010054
5. Dong W, Ding H. Full frequency de-noising method based on wavelet decomposition and noise-type detection. Neurocomputing 2016; 214: 902-909, https://doi.org/10.1016/j.neucom.2016.06.072
6. Dzierwa A, Galda L, Tupaj M, Dudek K. Investigation of wear resistance of selected materials after slide burnishing process. Eksploatacja i Niezawodnosc - Maintenance and Reliability 2020; 22(3): 432-439, https://doi.org/10.17531/ein.2020.3.5
7. Gomez C, Su R, Thompson A, DiSciacca J, Lawes S, Leach R K. Optimisation of surface measurement for metal additive manufacturing using coherence scanning interferometry. Optical Engineering 2017; 56(11): 111714, https://doi.org/10.1117/1.OE.56.11.111714
8. Haitjema H, Morel M A A. Method for approximate noise elimination in form and roughness measurements. In: Proceedings of SPIE 2003; 5190: 203-210.
9. Haitjema H. Uncertainty in measurement of surface topography. Surface Topography: Metrology and Properties 2015; 3(3): 035004, https://doi.org/10.1088/2051-672X/3/3/035004
10. Hart M, Vass D G, Begbie M L. Fast surface profiling by spectral analysis of white-light interferograms with Fourier transform spectroscopy. Applied Optics 1998; 37(10): 1764-1769, https://doi.org/10.1364/AO.37.001764
11. He Y F, Tang J Y, Zhou W, Liao D R. Research on the obtainment of topography parameters by rough surface simulation with fast Fourier transform. Journal of Tribology-Transactions of the ASME 2015; 137(3): 031401, https://doi.org/10.1115/1.4029843
12. ISO 2016 25178-600 Geometrical product specification (GPS) - Surface texture: Areal Part 600: Metrological characteristics for areal-topography measuring methods.
13. ISO 25178-3:2012 Geometrical product specifications (GPS) – Surface texture: Areal – Part 3: Specification operators.
14. ISO 25178-605 Geometrical product specification (GPS) – Surface Texture: Areal – Part 605: Nominal characteristics of non-contact (point autofocus probe) instruments, First Edition 2004.
15. Itoh T, Yamauchi N. Surface morphology characterisation of pentacene thin film and its substrate with under-layers by power spectral density using fast Fourier transform algorithms. Applied Surface Science 2007; 253(14): 6196-6202, https://doi.org/10.1016/j.apsusc.2007.01.056
16. Kiselev I, Kiselev E I, Drexel M, Hauptmannl M. Noise robustness of interferometric surface topography evaluation methods. Correlogram correlation. Surface Topography: Metrology and Properties 2017; 5(4): 045008, https://doi.org/10.1088/2051-672X/aa9459
17. Kubiak K J, Wilson M C T, Mathia T G, Carval Ph. Wettability versus roughness of engineering surfaces. Wear 2011; 271(3–4): 523-528, https://doi.org/10.1016/j.wear.2010.03.029

18. Lin C S, Yang S W, Lin H L, Li J W. Measurement of surface profile and surface roughness of fibre-optic interconnect by fast Fourier transform. Metrology and Measurement Systems 2017; 24(2): 381-390, https://doi.org/10.1515/mms-2017-0028
19. Liu S B, Wang Q. Studying contact stress fields caused by surface tractions with a discrete convolution and fast Fourier Transform algorithm. Journal of Tribology-Transactions of the ASME 2002; 24(1): 36-45, https://doi.org/10.1115/1.1401017
20. Magdziak M, Wdowik R. Coordinate Measurements of Geometrically Complex Ceramic Parts. Applied Mechanics and Materials 2014; 627: 172–176, https://doi.org/10.4028/www.scientific.net/AMM.627.172
21. Marinescu I D, Rowe W B, Dimitrov B, Ohmori H. Tribology of Abrasive Machining Processes. 2nd Edition. William Andrew Publishing, Norwich, NY, 2013, https://doi.org/10.1016/C2010-0-67070-2
22. Pawlus P, Reizer R, Wieczorowski M. Comparison of results of surface texture measurement obtained with stylus methods and optical methods. Metrology and Measurement Systems 2018; 25(3): 589–602, https://doi.org/10.24425/123894
23. Pawlus P. Digitisation of surface topography measurement results. Measurement 2007; 40(6): 672-686, https://doi.org/10.1016/j.measurement.2006.07.009
24. Pawlus P. The errors of surface topography measurement using stylus instruments. Metrology and Measurement Systems 2002; 9(3): 273-289.
25. Płonka S, Zaborski A. Operational wear of the neck of spindle coating in cooperation with yarn. Eksploatacja i Niezawodnosc - Maintenance and Reliability 2015; 17(4): 496–503, https://doi.org/10.17531/ein.2015.4.3
26. Podulka P. Bisquare robust polynomial fitting method for dimple distortion minimisation in surface quality analysis. Surface and Interface Analysis 2020; 52(12) 875–881, https://doi.org/10.1002/sia.6793
27. Podulka P. Comparisons of envelope morphological filtering methods and various regular algorithms for surface texture analysis. Metrology and Measurement Systems 2020; 27(2): 243-263, https://doi.org/0.24425/mms.2020.132772
28. Podulka P. Edge-area form removal of two-process surfaces with valley excluding method approach. MATEC web of conferences 2019; 252: 05020, https://doi.org/10.1051/matecconf/201925205020
29. Podulka P. Proposal of Frequency-Based Decomposition Approach for minimisation of errors in surface texture parameter calculation. Surface and Interface Analysis 2020; 52(12) 882–889, https://doi.org/10.1002/sia.6840
30. Podulka P. The effect of valley depth on areal form removal in surface topography measurements. Bulletin of the Polish Academy of Sciences. Technical Sciences 2019; 67(2): 391-400, https://doi.org/10.24425/bpas.2019.128597
31. Podulka P. The effect of valley location in two-process surface topography analysis. Advances in Science and Technology Research Journal 2018; 12(4): 97-102, https://doi.org/10.12913/22998624/100343
32. Raja J, Muralikrishnan B, Fu S. Recent advances in separation of roughness, waviness and form. Precision Engineering 2002; 26(2): 222-235, https://doi.org/10.1016/S0141-6359(02)00103-4
33. Raja J, Radhakrishnan V. Filtering of surface profiles using fast Fourier transform. International Journal of Machine Tools & Manufacture 1979; 19: 133–141, https://doi.org/10.1016/0020-7357(79)90003-9
34. Rhee H G, Vorburger T V, Fu J, Renegar T B, Song J F. Comparison of roughness measurements obtained with optical and stylus techniques. Proceedings of the 10th International Conference on Metrology and Properties of Engineering Surfaces, Saint-Etienne, France, 2005, pp. 39–47.
35. Sainsot P, Lubrecht A A. Efficient solution of the dry contact of rough surfaces: a comparison of fast Fourier transform and multigrid methods. Proceedings of the Institution of Mechanical Engineers, Part J: Journal of Engineering Tribology 2011; 225(6): 441-448, https://doi.org/10.1177/1350650111401535
36. Schmehl R, Nebeker B M, Hirleman E D. Discrete-dipole approximation for scattering by features on surfaces by means of a two-dimensional fast Fourier transform technique. Journal Of The Optical Society Of America A-Optics Image Science And Vision 1997; 14(11): 3026-3036, https://doi.org/10.1364/JOSAA.14.003026
37. Thomas T R. Rough Surfaces. Second Edition, Imperial College Press, London, 1999.
38. Tien C L, Yang H M, Liu M C. The measurement of surface roughness of optical thin films based on fast Fourier transform. Thin Solid Films 2009; 517(17): 5110–5115, https://doi.org/10.1016/j.tsf.2009.03.193
39. Vo Q, Fang F, Zhang X, Gao H. Surface recovery algorithm in white light interferometry based on combined white light phase shifting and fast Fourier transform algorithms. Applied Optics 2017; 56(29): 8174-8185, https://doi.org/10.1364/AO.56.008174
40. Vorburger T V, Rhee H G,Renegar T B, Song J F, Zheng A. Comparison of optical and stylus methods for measurement of surface texture. The International Journal of Advanced Manufacturing Technology 2007; 33: 110–118, https://doi.org/10.1007/s00170-007-0953-8
41. Wang C, D-Amato R, Gomez E. Confidence Distance Matrix for outlier identification A new method to improve the characterisations of surfaces measured by confocal microscopy. Measurement 2019; 137: 484-500, https://doi.org/10.1016/j.measurement.2019.01.043
42. Wang Y, Liu Y, Zhang G, Wang Y. A simulation method for non-Gaussian rough surfaces using Fast Fourier Transform and translation process theory. Journal of Tribology-Transactions of the ASME 2018; 140(2) 021403, https://doi.org/10.1115/1.4037793
43. Wang Y, Yuan P, Ma J, Qian L. Scattering noise and measurement artifacts in a single-shot cross-correlator and their suppression. Applied Physics B 2013; 111: 501–508, https://doi.org/10.1007/s00340-013-5364-y
44. Wdowik R, Magdziak M, Porzycki J. Measurements of surface roughness in ultrasonic assisted grinding of ceramic materials. Applied Mechanics and Materials 2014; 627: 191–196, https://doi.org/10.4028/www.scientific.net/AMM.627.191
45. Zhang H, Yuan Y, Piao W. A universal spline filter for surface metrology. Measurement 2010; 43(10): 1575-1582, https://doi.org/10.1016/j.measurement.2010.09.008